19th Australasian Fluid Mechanics Conference
Melbourne, Australia
8-11 December 2014

Quasi-Two-Dimensional MHD Duct Flow Around a 180-Degree Sharp Bend in a Strong Magnetic Field

A. M. Sapardi[1,2], W. K. Hussam[1], A. Pothérat[3] and G. J. Sheard[1]

[1]The Sheard Lab, Department of Mechanical and Aerospace Engineering, Monash University, Victoria 3800, Australia

[2]Department of Mechanical Engineering, International Islamic University Malaysia, Kuala Lumpur 53300, Malaysia

[3]Applied Mathematics Research Centre, Coventry University, Coventry CV1 5FB, United Kingdom

Abstract

This study considers the quasi-two-dimensional flow of an electrically conducting fluid subjected to a strong out-of-plane magnetic field in a rectangular duct. The effect of Hartmann number on flow features such as the length of the downstream recirculation bubbles and the threshold Reynolds numbers between steady-state and unsteady flow regimes for values of the ratio between the throat of the bend and the duct height, $\beta = 1$ are identified. The simulations reveal that the primary recirculation bubble length decreases with increasing Hartmann number, and simultaneously the secondary recirculation bubble is significantly damped compared to the corresponding non-MHD case. The critical Reynolds number where the transitions from steady to unsteady flow occurs was found to increase with increasing of Hartman number. This study provides information that will be useful for refining the design of heat exchanger ducting in MHD systems to maximise the useful mass transport adjacent to the duct walls where heating is applied.

Introduction

The flow of liquid metal in ducts in the presence of a transverse magnetic field has received attention because of its importance in applications such as metallurgical processing, flow pumps and blood flow meters. Magnetic confinement fusion reactors are the primary application motivating this study. In these reactors, liquid metal flowing through ducts within blankets surrounding the reactor in the presence of strong magnetic fields is used as a coolant and as a breeder. The motion of liquid metal in a strong magnetic field induces eddy current, which in turn interacts with the magnetic field producing a Lorentz force. This force has a substantial impact on the turbulence characteristics, and employs an inhibiting force on fluctuations parallel to the magnetic field. Further, under conditions where the magnetic field is strong, uniform and acting perpendicular to the plane of the duct bend, the flow is expected to become highly two-dimensional in the core of the duct, and therefore it may be efficiently modelled using the quasi-two-dimensional model proposed by Sommeria and Moreau [6].

The 180-degree sharp bend geometry is an integral feature of the ducting within prototype fusion reactor blankets. The abrupt change of the sharp bend causes flow separation which has the potential to enhance the heat transfer process, but work is needed to understand the effect of Hartmann braking on the flow under the magnetic field. Most studies up to now have focused only on non-MHD problems such as the effect of sharp bend on the dynamics of the flow [7], heat transfer in a sharp bend [1] and the effect turn region on the pressure loss distribution [5], and this is the first to tackle the MHD problem.

This problem is computed using a two-dimensional spectral-element incompressible flow solver augmented with the linear Hartmann friction term to satisfy the quasi-two-dimensional model. The two-dimensional steady flow structure in the downstream duct is found to have similarities with the flow over backward facing step: the flow first passes over a large recirculation bubble attached to the downstream side of the inner corner of the bend, and subsequently a secondary recirculation bubble develops on the outer wall a little further downstream.

Numerical Methodology

Viscous fluid is considered to be in motion in a duct with a sharp 180-degree bend with the middle of the inner wall of the turning part located at the origin. We take the flow direction to be such that fluid past around the sharp bend, with the upstream and downstream ducts parallel to each other. The flow is assumed to have constant density ρ and constant kinematic viscosity ν.

Figure 1 illustrates the computational domain under consideration including the geometric parameters for the problem. The channel widths in the inlet and at the bend are represented by a and b, respectively. The height of the inlet and outlet are identical. The divider thickness is represented by c with d and e denoting the lengths of bottom and top boundaries. The ratio c/a is set to 0.04, while the lengths of the bottom and top boundaries determined by $(d-b)/a = 15$ and $e/d = 3$. The opening ratio of the bend is represented by $\beta = b/a$. Fluid enters from the inlet and flows downstream past the sharp bend towards the outlet channel.

There are three non-dimensional numbers which are used to characterize MHD flows. First, the Reynolds number,

$$Re = U_o a/\nu, \tag{1}$$

where a is a characteristic length scale of the motion, which in this study is the inlet height, U_o is the maximum inlet velocity, and ν is the kinematic viscosity of the fluid. Second is Hartmann number (square root of the ratio of Lorenz forces to viscous forces),

$$Ha = L_z B\sqrt{\frac{\sigma_e}{\rho\nu}}, \tag{2}$$

and third is the interaction parameter (the ratio of Lorentz forces to inertia),

$$N = \frac{\sigma_e B^2 L_z}{\rho U_o}, \tag{3}$$

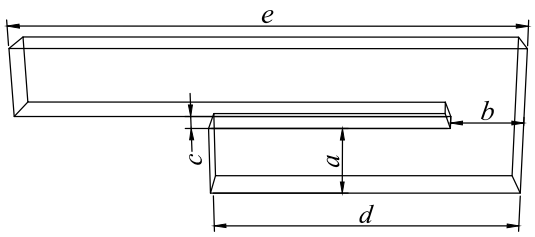

Figure 1. Flow geometry for the 180-degree sharp bend.

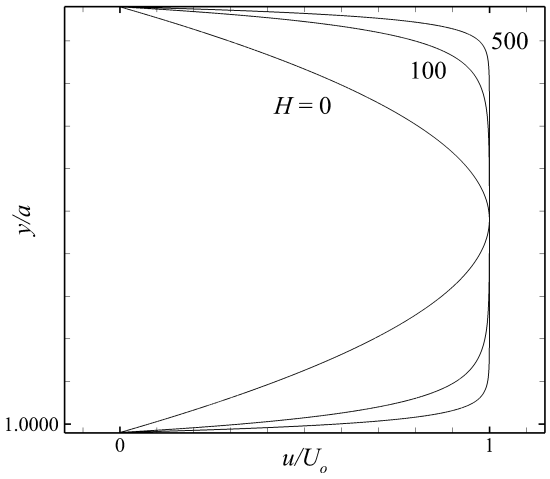

Figure 2. Normalized base flow velocity profile at H as indicated.

where B, ρ, σ_e and L_z are the magnetic field strength, mass density, electrical conductivity and the domain length in magnetic field direction, respectively. The interaction parameter can also be interpreted in terms of Ha and Re as $N = Ha^2/Re$. Due to large Ha and N values in magnetic confinement fusion applications, the flow is quasi-2D with a core region where the velocity is constant along the magnetic field direction, and thin Hartmann layers at the walls perpendicular to the magnetic field direction. Under these assumptions, Sommeria and Moreau [6] have derived a 2-D flow model by averaging the flow equations along the direction of the magnetic field.

$$\frac{\partial \mathbf{u}}{\partial t} = -(\mathbf{u}\cdot\nabla)\mathbf{u} - \nabla p + \frac{1}{Re}\nabla^2\mathbf{u} - \frac{H}{Re}\mathbf{u}, \tag{4}$$

$$\nabla\cdot\mathbf{u} = 0, \tag{5}$$

where $\mathbf{u}$ is the velocity averaged across the duct along the magnetic field and p is the static pressure The parameter $H = n(a^2/L_z^2)L_zB\sqrt{\sigma_e/(\rho\nu)}$ is a measure of the friction term representing the Lorentz force effect on the flow, n represents the number of Hartmann layers, which is in this case $n = 4$ [4].

Boundary conditions are imposed on the flows as follows. At the inflow boundary ($x = b-d, -1.02 \le y \le -0.02$), we impose Hartmann velocity profile [4] as shown in figure 2. As H approaches zero (non-MHD), this velocity profile reverts to two-dimensional Poiseuille velocity profile, while high values of H give an almost flat profile except at the vicinity of the wall which is in the Shercliff boundary layer with the thickness of $\delta_{Sh} = Ha^{-1/2}$.

Due to viscosity, velocity is zero at the interface between the wall and the fluid, hence the boundary conditions are the no-slip condition ($\mathbf{u} = 0$) at the wall. At the outflow boundary ($x = b-e, 0.02 \le y \le 1.02$), we impose a standard boundary condition for pressure: $p = 0$.

Computational Methods

Code Validation

The length of the outflow domain was tested to ensure it was sufficiently long to confirm that the results are independent of outflow effects. A convergence study determined acceptable outflow lengths between $20a \le e-b \le 100a$ by using the primary recirculation bubble as the convergence criteria. Hence, outflow length $e-b = 47a$ is used as it yields only 0.0002% error compared to the longest outflow length studied. From observations, the streamlines break away from the boundary when a boundary layer develops near the surface of an abrupt geometry change. Typical velocity profile near the point of separation demonstrates that it is possible to determine the point of separation and reattachment with points where the streamwise velocity is constant with respect to transverse direction:

$$\left.\frac{\partial u}{\partial y}\right|_x = 0. \tag{6}$$

The distance between separation and reattachment points represents the length of recirculation bubble. The code is validated by comparing the primary recirculation bubble length L_R/a obtained in non-MHD flow with $100 \le Re \le 700$ in this study with the results acquired by Zhang and Pothérat [7] and Chung *et al.*[1], which have discrepancies as small as 2.2% and 0.2%, respectively.

Mesh Resolution

Flow past a 180-degree sharp bend is a deceptively difficult problem to fully resolve, especially at large Re number. This section describes the tests used to validate the numerical algorithm, and to select appropriate meshes and element order. The spatial resolution study varied the order of interpolation within each macro-element of a mesh based on domain length parameters from the mesh domain. For consistency with the domain size, the mesh employed in this study models a 180-degree sharp bend with opening ratio $\beta = 1$.

The mesh is structured and is refined in the vicinity of the inner wall of the sharp bend and in the downstream duct in order to capture the unique structure of the flow downstream of the bend. Computations have been performed using spectral elements with polynomial degrees varying from $N = 4$ to 8.

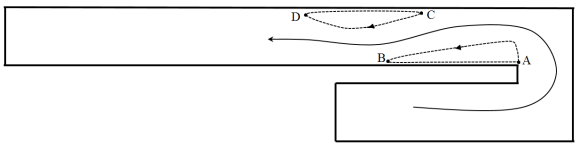

Figure 3. Sketch of separation and re-attachment points defining the locations of all recirculations. Reproduced from Zhang & Pothérat [7].

To demonstrate the accuracy of computing recirculation length in the base flow, we present table 1 as a function of polynomial order and base flow. The recirculation length was computed at $Re = 500$ with $\beta = 1$ which is steady-state and has two recirculation bubbles at the downstream end of the duct illustrated in figure 3. From the relative error, it was decided that the polynomial order $N = 5$ would be used hereafter.

Results

Recirculation Bubbles

Simulations were conducted at Hartmann ranging from $H = 0$ to $H = 500$ at increment of 100, and at a range of Reynolds numbers for each H. Figure 4 shows the effect of the strong spanwise magnetic field on the structure of the liquid metal flow around the bend, especially on the recirculation bubbles. As the strength of the magnetic field increases, the length of both the primary and secondary recirculation bubbles decrease. It is further apparent that beyond a critical Hartmann number, the secondary bubble disappears because the extra dissipation delays

N	A	B	C	D	L_{R1}/a	L_{R2}/a	%diff L_{R1}/a	% diff L_{R2}/a
4	0	-4.80573	-3.70773	-9.77262	4.805727	6.064888	0.03071	0.07967
5	0	-4.80716	-3.7069	-9.77645	4.807159	6.069547	0.00092	0.00292
6	0	-4.8073	-3.70705	-9.77667	4.807295	6.069618	0.00192	0.00175
7	0	-4.80725	-3.70701	-9.77667	4.807248	6.069661	0.00094	0.00104
8	0	-4.8072	-3.70697	-9.77669	4.807203	6.069724	-	-

Table 1: Dependence of recirculation length on polynomial order. Parameter N indicates the independent polynomial order of the base flow. Two separation points (A and C) and two reattachment points (B and D) as indicated in figure 3 computed on the mesh at $Re = 500$ and $\beta = 1$ are given. L_{R1}/a and L_{R2}/a represent the recirculation length of primary and secondary recirculation bubbles, respectively.

the appearance of the secondary recirculation significantly that it reaches a point where the first recirculation becomes unstable without the second having formed yet. Increasing Re acts to increase the recirculation bubble length. The recirculation length is calculated by finding the distance between the separation and reattachment points using equation (6). The length of recirculation bubble was recorded at a large number of points in the Re-H parameter space (Figure 5). L_{R1}/a increases linearly with increasing Re for a constant H, and decreases with H for a constant Re. For the non-MHD case, the L_{R1}/a increases significantly slower when the secondary recirculation bubble starts to appear, but the effect of the secondary recirculation bubble is not noticeable in the MHD flows because the secondary recirculation bubble is damped significantly under the presence of high magnetic field.

A non-linear optimization was performed to find exponents A and B to maximize the square of the correlation coefficient (R^2) of a linear least-squares fit to the L_{R1}/a data when plotted against $Re^A H^B$. To two decimal places, the optimal exponents were determined to be $A = 1$ and $B = -2/3$ with $R^2 = 0.9976$. This implies that decreasing H has a similar effect to increasing Re in primary bubble formation which may affect the tendency of the flow to destabilise. Dousset and Pothérat [2], in their study in flow around a cylinder under a strong axial magnetic field with blockage ratio $B = 0.25$, found that the recirculation bubble length behind the cylinder L_R/d data collapsed when plotted against $Re/H^{4/5}$, meanwhile Hussam *et al.*[3] proposed a more general relationship incorporating the blockage ratio against scaling $Re^{0.844}H^{-0.711}B^{0.166}$. Here, the universal relationship between the primary recirculation bubble length, Re and H is approximated by

$$L_{R1}/a = 0.1361 Re H^{-2/3} - 0.124, \qquad (7)$$

and the agreeable collapse of the data obtained is shown in figure 6.

Equation (7) can be used to approximate at what value of Re and H the primary recirculation bubble is expected to appear (i.e. by solving for $L_{R1}/a = 0$). This gives

$$Re = 0.911 H^{2/3}. \qquad (8)$$

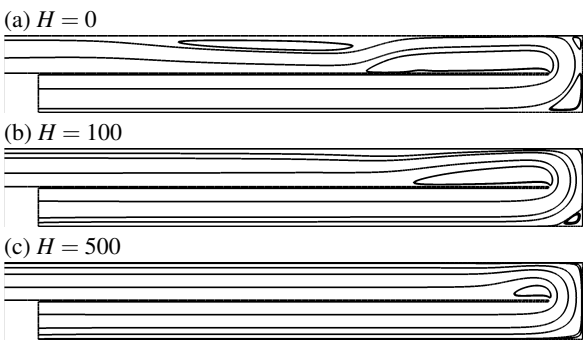

Figure 4. Streamlines of steady flow for $Re = 700$, $0 \leq H \leq 500$.

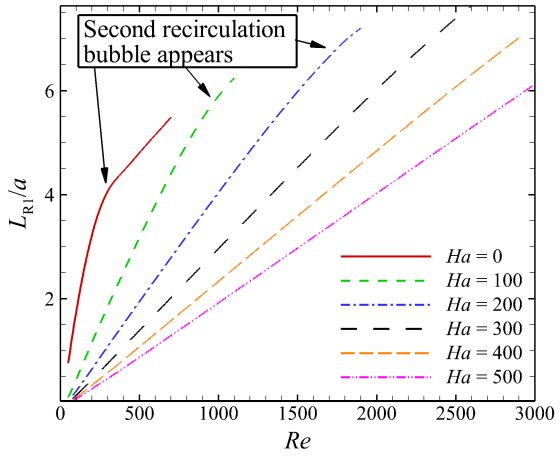

Figure 5. Primary recirculation bubble length in the function of Re.

Critical Reynolds Number

Figure 7 shows the effect of H on contours of vorticity at $Re = 1500$. It is apparent that the flow at higher H is more stable, as an example, the stronger magnetic field in $H = 200$ (Figure 7(b)) sustains the flow steadiness, whereas the flow at $H = 100$ (Figure 7(a)) is unsteady.

Figure 8 shows the critical Reynolds number, Re_c as a function of H. For $\beta = 1$, Re_c is found to increase with increasing H. This is due to the effect of H which delays the transition from steady to unsteady regimes, causing the greater stability of the flow. Higher H acts to diminish the recirculation bubbles, which delays the transition, resulting in a higher Re being required to invoke transition. Other than that, a higher value of Re also must be reached to trigger the appearance of the primary and secondary recirculation bubbles when H increased. The Reynolds number to trigger the primary recirculation bubble Re_{R1} is not significantly affected by H, as presented in the approximated equation (8) and long-dashed black line in figure 8. However, the appearance of the secondary recirculation bubble is significantly delayed as H increased. As H increased, the secondary recirculation bubble length is damped and appeared shortly before the flow becomes unsteady. The secondary recirculation bubble does not appear at all for $H \geq 316$.

According to Zhang and Pothérat [7], both bubbles play important role in the transition of the non-MHD flow due to the instability generated by the shear layer in the main stream

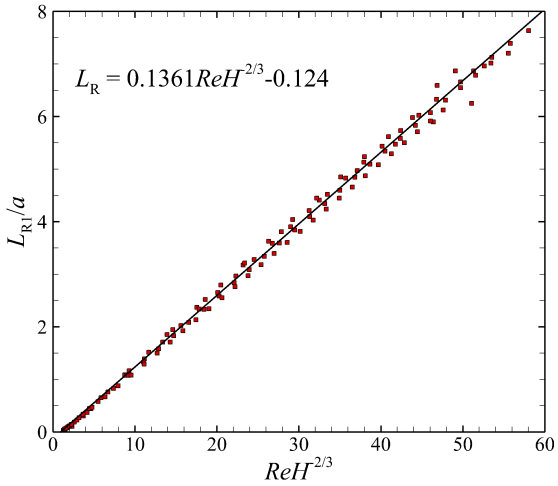

Figure 6. Collapse of recirculation bubble length over ranges of $100 \leq H \leq 500$ and $50 \leq Re \leq 2500$.

between both bubbles. As for the MHD flow, increasing H inhibits the formation of the secondary recirculation bubble, hence the instability for $H \geq 317$ is due to a different mechanism which occurs in the primary recirculation bubble vicinity as suggested in figure 9 by the shedding of vorticity immediately behind the bend. Here the primary bubble is obliterated.

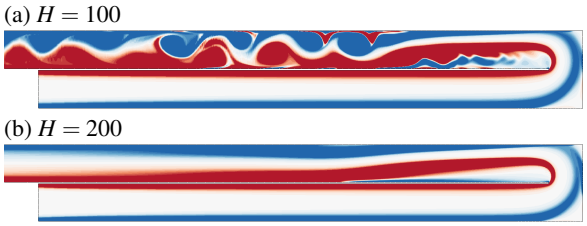

Figure 7. Vorticity contours for $Re = 1500$, (a) $H = 100$ and (b) $H = 200$. Note that at $Re = 1500$, $0 \leq H \leq 100$ is unsteady, $H \geq 200$ is steady.

Conclusions

We have studied the flow of a liquid metal around a 180-degree sharp bend under a strong homogeneous magnetic field aligned with the spanwise direction of the flow. The flow can be assumed to be quasi-2D using SM82 [6] due to the high values of N and H. The recirculation bubbles along the downstream duct are damped as H increased, especially the secondary recirculation bubble. Beyond $H \approx 317$, the secondary recirculation bubble fails to form making the flow directly become unsteady without its presence. This suggest a different mechanism of instability to that observed in non-MHD flow. The critical Reynolds number for the transition from steady to unsteady flow at different H and $\beta = 1$ was determined and it was found that Re_c increases with increasing H.

Acknowledgements

This research was supported by ARC Discovery Grant DP120100153, high-performance computing time allocations from the National Computational Infrastructure (NCI) and the Victorian Life Sciences Computation Initiative (VLSCI), and the Monash SunGRID. A.M.S. is supported by Ministry of Education Malaysia and International Islamic University Malaysia.

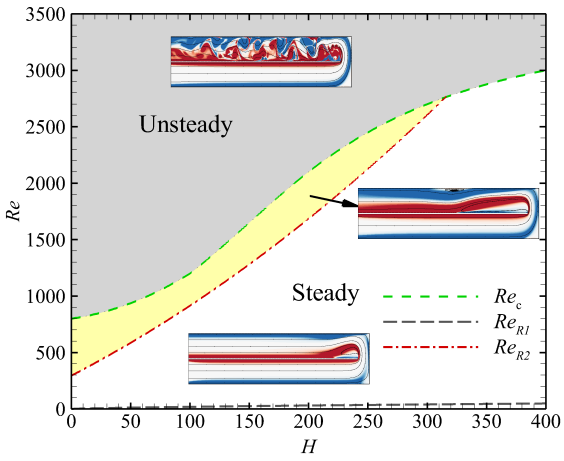

Figure 8. Critical Reynolds number where transitions from steady to unsteady, and Re when the secondary recirculation bubble starts to appear for $0 \leq H \leq 400$. The grey region indicates unsteady regime, the regions below the dashed-green line is steady regimes, while the yellow region is where the primary and secondary recirculation bubbles coexist in the downstream duct.

Figure 9. Unsteady flow at $H = 400$, $Re = 3000$ without the presence of secondary recirculation bubble prior to Re_c.

References

[1] Chung, Y. M., Tucker, P. G. and Roychowdhury, D., 2003, Unsteady laminar flow and convective heat transfer in a sharp 180 bend, *International journal of heat and fluid flow*, **24**, 67–76.

[2] Dousset, V. and Pothérat, A., 2008, Numerical simulations of a cylinder wake under a strong axial magnetic field, *Physics of Fluids*, **20**, 017104.

[3] Hussam, W. K., Thompson, M. C. and Sheard, G. J., 2012, Optimal transient disturbances behind a circular cylinder in a quasi-two-dimensional magnetohydrodynamic duct flow, *Physics of Fluids*, **24**, 024105.

[4] Pothérat, A., 2007, Quasi-two-dimensional perturbations in duct flows under transverse magnetic field, *Physics of Fluids*, **19**, 074104.

[5] Rao, D., Babu, C. S. and Prabhu, S., 2004, Effect of turn region treatments on the pressure loss distribution in a smooth square channel with sharp 180 bend, *International Journal of Rotating Machinery*, **10**, 459–468.

[6] Sommeria, J. and Moreau, R., 1982, Why, how, and when, MHD turbulence becomes two-dimensional, *Journal of Fluid Mechanics*, **118**, 507–518.

[7] Zhang, L. and Pothérat, A., 2013, Influence of the geometry on the two-and three-dimensional dynamics of the flow in a 180 sharp bend, *Physics of Fluids*, **25**, 053605.